OPEN ACCESS

University of BRISTOL

Roettger, K., Marroux, H., Chemin, A., Elsdon, E., Oliver, T. A. A., Street, S., Henderson, A. S. J., Galan, C., Orr-Ewing, A., & Roberts, G. (2017). Is UV-Induced Electron-Driven Proton Transfer Active in a Chemically Modified A•T DNA Base Pair? *Journal of Physical Chemistry B*, *121*(17), 4448-4455. https://doi.org/10.1021/acs.jpcb.7b02679

Peer reviewed version

License (if available):
CC BY-NC

Link to published version (if available):
10.1021/acs.jpcb.7b02679

Link to publication record in Explore Bristol Research
PDF-document

This is the author accepted manuscript (AAM). The final published version (version of record) is available online via ACS at http://pubs.acs.org/doi/abs/10.1021/acs.jpcb.7b02679. Please refer to any applicable terms of use of the publisher.

University of Bristol - Explore Bristol Research
General rights

This document is made available in accordance with publisher policies. Please cite only the published version using the reference above. Full terms of use are available:
http://www.bristol.ac.uk/red/research-policy/pure/user-guides/ebr-terms/

Is UV-Induced Electron-Driven Proton Transfer Active in a Chemically Modified A•T DNA Base Pair?

Katharina Röttger, Hugo J. B. Marroux, Arsène F. M. Chemin, Emma Elsdon, Thomas A. A. Oliver, Steven T. G. Street, Alexander S. Henderson, M. Carmen Galan, Andrew J. Orr-Ewing* and Gareth M. Roberts*

School of Chemistry, University of Bristol, Cantock's Close, Bristol, BS8 1TS, UK

*Correspondence to: g.m.roberts@bristol.ac.uk; a.orr-ewing@bristol.ac.uk

Abstract

Transient electronic and vibrational absorption spectroscopies have been used to investigate whether UV-induced electron-driven proton transfer (EDPT) mechanisms are active in a chemically modified adenine-thymine (A•T) DNA base pair. To enhance the fraction of biologically relevant Watson-Crick (WC) hydrogen-bonding motifs, and eliminate undesired Hoogsteen structures, a chemically modified derivative of A was synthesized, 8-(*t*-butyl)-9-ethyl-adenine (8tBA). Equimolar solutions of 8tBA and silyl-protected T nucleosides in chloroform yield a mixture of WC pairs, reverse WC pairs and residual monomers. Unlike previous transient absorption studies of WC guanine-cytosine (G•C) pairs, no clear spectroscopic or kinetic evidence was identified for the participation of EDPT in the excited state relaxation dynamics of 8tBA•T pairs, although ultrafast (sub-100 fs) EDPT cannot be discounted. Monomer-like dynamics are proposed to dominate in 8tBA•T.

1. Introduction

Over five decades ago, Löwdin recognized that Watson-Crick (WC) base pairing opens the possibility for proton or hydrogen (H) atom transfer across the intermolecular H-bonds of DNA.[1] This seminal work proposed that such behavior could offer a route to mutation by generating so-called 'rare' nucleobase tautomers within the double helix. In its most recent guise, the debate surrounding H-atom transfer in DNA has predominately stemmed from theoretical studies, which instead postulated that ultrafast interstrand electron-driven proton transfer (EDPT) – inter-base electron-transfer followed by proton transfer,[2] resulting in the net exchange of a H-atom – contributes to the prevention of mutagenic photolesions in DNA excited by absorption of UV radiation.[3-6] Despite extensive prior study of DNA photodynamics,[6-9] the question of whether UV-induced EDPT is active in WC base pairs has until very recently remained contentious from an experimental perspective.[10-16]

Experimentally, guanine-cytosine (G•C) WC pairs have received the most attention with respect to EDPT dynamics.[10, 11, 14, 16-18] Recent ultrafast transient electronic absorption spectroscopy (TEAS) and transient vibrational absorption spectroscopy (TVAS) results from our research group revealed that, following 260 nm excitation, G•C WC pairs in chloroform undergo a sequence of EDPT processes within 2.9 ps, forming a double H-atom transferred photoproduct with a quantum yield of ≤10%.[14] These findings verified predictions from a number of prior computations.[3, 19-21] TVAS measurements by both Bucher *et al*.[12] and Zhang *et al*.[13, 15] investigated the role of EDPT pathways in DNA duplexes in aqueous solution. The latter study concluded that, for duplexes containing only G•C pairs, a 'hybrid' EDPT process occurs, involving interstrand proton transfer after initial UV-induced intrastrand, inter-base charge-transfer (CT).[13, 15] Very recently, Zhang *et al*. also postulated that purely interstrand EDPT could be active in chemically modified, cyclic DNA mini-duplexes containing G•C.[16] This purely interstrand process is akin to the first ultrafast EDPT step observed in individual G•C WC pairs,[14] and the results highlight that both base pair sequence and local structure within the duplex play a critical role in determining the nature of UV-induced EDPT processes for natural DNA.

Analogous to G•C, theoretical studies have also predicted that both single and/or sequential double EDPT pathways may be active in individual adenine-thymine (A•T) WC pairs after UV excitation.[5, 22-27] However, unlike G•C, there is some debate regarding the stability of the imino-enol tautomer pair of A•T resulting from double H-atom transfer[23, 28] and whether EDPT is enhanced when A•T is placed in polar solvents.[6] Zhang *et al*. invoked hybrid EDPT pathways to be active in DNA duplexes containing only A•T,[13] but the role and dynamics of EDPT across H-bonds in individual, solvated A•T WC base pairs remain experimentally unexplored. The origins of this apparent oversight predominantly lie in the fact that, upon solvation in aprotic solvents (which encourages inter-base H-bonding[10]), an equimolar mixture of A and T nucleosides associate to form a selection of base pairing motifs (*cf*. Figure 1): WC (**1**), reverse WC (**2**), Hoogsteen (**3**) and reverse Hoogsteen (**4**).[29] For solution-phase transient absorption methods, this behavior prevents extraction of information purely related to the biologically relevant WC structure, instead returning an ensemble observation of the dynamics from all four species.

Herein, we report the first TEAS and TVAS measurements on a chemically modified A•T WC base pair, solvated in chloroform solution, which eliminates formation of undesired Hoogsteen-type structures. Using this model A•T pair system, we gain the first experimental insights into whether EDPT is active in UV-excited A•T, and directly compare and contrast the findings from these results with our previous studies on G•C WC pairs in chloroform[14] and published theoretical work on A•T.[5, 22-28]

2. Methods

A. Synthesis

The investigated T and 2'-deoxy-adenosine (dA) nucleosides were protected by bulky, apolar *t*-butyldimethylsilyl (TBDMS) groups to ensure a sufficient solubility in chloroform, henceforth simply termed T and dA. The synthesis has previously been described in detail.[14, 30] Synthesis and characterization of a chemically modified adenine derivative, 8-(*t*-butyl)-9-ethyl-adenine (8tBA – Figure 1), is described in detail in the online Supporting Information (SI).

B. Transient Absorption Spectroscopy

TEAS and TVAS experiments were performed using an apparatus that has been described previously.[31] The system consists of a regenerative amplifier (Coherent Legend Elite HE+), operating at 1 kHz and producing 40 fs pulses at 800 nm (5 W). This fundamental beam is split into three parts using a series of beam splitters: two parts have energies of 2.45 mJ/pulse, with one much lower energy beam of 100 μJ/pulse. The two 2.45 mJ/pulse beams seed two Coherent OPerA Solo optical parametric amplifiers (OPAs). One of these OPAs produces spectrally tunable light spanning the UV to infrared (IR) range and is used to generate the 260 nm (~100 fs, ~0.6 – 1 μJ/pulse) pump pulses for all our transient absorption experiments. The remaining OPA was used to generate broadband (~300 cm^{-1}) IR pulses, centered at ~1680 cm^{-1}, for use as our probe in TVAS experiments, with energies of ~1 μJ/pulse at the sample. Finally, the remaining 100 μJ/pulse 800-nm seed is used to generate a broadband white-light continuum (WLC), which spans wavelengths from ~330 nm to >800 nm, for use as the probe in TEAS experiments.

For TEAS, polarization of the WLC probe pulse was maintained at the magic angle (54.7°), relative to the UV pump pulse polarization by using a λ/2 waveplate in the 800 nm WLC seed beam line. After transmission through the sample, the WLC probe and signal was collimated and focused into a spectrograph (Andor, Shamrock 163) coupled to a 1024 element photodiode array (Entwicklungsbüro Stresing). The spectrometer can disperse 750 – 260 nm probe wavelengths on the detector attaining a spectral resolution of ~0.5 nm. Prior to interaction with the sample, the UV pump beam was modulated at 500 Hz (blocking every other pulse) with an optical chopper wheel (Thorlabs, MC2000) to obtain sequential pump on/off spectra pairs at each pump-probe time delay (*t*), which are required to generate the individual transient absorption spectra. Data acquisition and calculation of the transient absorption spectra at each *t* was carried out using a custom built LabVIEW program. *t* was controlled by changing the path length of the pump beam with an aluminum retro-reflector (PLX) mounted on a motorized 220 mm delay stage (Thorlabs, DDS220/M), providing a maximum possible delay of $t = 1.3$ ns. Non-resonant two-color two-photon absorption measurements in D_2O reveal an instrument response function (IRF) of ~110-120 fs in our TEAS measurements.[31]

For TVAS, the IR probe was reflectively focused into the sample, so that the probed region of the sample was uniformly excited by the more loosely focused UV pump beam. After passing through the sample, the transmitted IR probe light was detected by a 128 pixel, liquid N_2 cooled Mercury Cadmium Telluride array (Infrared Associates Inc., MCT-10-128) coupled to a spectrometer (HORIBA Scientific, iHR320), providing a spectral resolution of ~2 cm^{-1}.

Sample solutions of 8tBA (c_0 = 50 mM), dA (c_0 = 50 mM), T (c_0 = 50 mM) and equimolar mixtures of 8tBA and T (c_0 = 50 mM) were prepared in anhydrous $CHCl_3$ (Sigma-Aldrich, 99.99%). These sample solutions were then delivered through a stainless steel flow cell, containing two 1.5 mm thick CaF_2 windows separated by a 380 μm thick Teflon spacer, which defined the absorption path length. The sample solution was flowed continuously through the cell by a peristaltic pump (Cole Parmer, Masterflex) with PTFE tubing throughout. All measurements were repeated at least two times on a single day and at least two times on different days with fresh sample solution to ensure reproducibility.

C. Computational Calculations

Ground state density functional theory (DFT) calculations were performed to determine the relative energies (ΔE) and Boltzmann populations (P_B) at 298K for 8tBA•T and A•T base pairs in their Watson-Crick, reverse Watson-Crick, Hoogsteen and reverse Hoogsteen configurations. Methyl groups were used in place of the 2'-deoxy-ribose groups for computational expediency (Figure 1, R = CH_3). The structures for these species, calculated at the B3LYP/6-311++G** level of theory in Gaussian 09,[32] are shown in Figure S1. A polarizable continuum model (PCM) was used to capture the dielectric effects of the chloroform solvent. Harmonic frequencies were calculated and all simulated FTIR spectra were scaled by a factor of 0.983. Simulated vibrational spectra were constructed by convolution of the vibrational 'stick' spectra with Gaussian functions with 25 cm^{-1} full-width at half maximum in the carbonyl stretching region. Our chosen method is benchmarked by comparing simulated FTIR spectra for the 8tBA•T pairs with the experimentally extracted FTIR spectrum (see Figure 4c), which demonstrated good agreement between experiment and theory. Analogous theoretical

methods were also used previously to model the photochemistry of G•C base pairs in chloroform.[14]

3. Results & Analysis

In order to remove contributions from Hoogsteen-type motifs, we synthesized a chemically modified derivative of adenine, 8-(*t*-butyl)-9-ethyl-adenine (8tBA). The presence of the bulky *t*-butyl group in the C_8-position of 8tBA eliminates formation of Hoogsteen H-bonding configurations (**3**, **4**) upon association with silyl-protected T nucleosides (Figure 1).[33] Similar approaches to eliminating Hoogsteen structures in related A•U pairs were demonstrated previously, albeit with a more-perturbing, UV-absorbing phenyl ring in the C_8-position.[34] The dominance of structures **1** and **2** for 8tBA•T pairs in chloroform is supported by DFT calculations, which we have used together with NMR and two-dimensional infrared spectroscopy to characterize our samples (see SI). This conclusion is highlighted in Table 1, which shows the calculated (B3LYP/6-311++G**) Boltzmann populations at 298 K (P_B) and relative energies (ΔE) for H-bonding configurations **1**-**4** of 8tBA•T, relative to A•T, in chloroform.

As shown for related systems in chloroform,[10, 35, 36] the propensity for 8tBA and T to associate can be described by a solvent-dependent equilibrium constant, $K_{8tBA\bullet T}$ = [8tBA•T]/[8tBA][T]. The degree of association, $\beta_{8tBA\bullet T}$, at a given concentration, c_0, is subsequently obtained *via* the relationship $K_{8tBA\bullet T} = \beta_{8tBA\bullet T}/c_0(1-\beta_{8tBA\bullet T})^2$, where c_0 = [8tBA] + [T] + [8tBA•T]. $K_{8tBA\bullet T}$ can be obtained through an analysis of concentration dependent steady state FTIR spectra recorded in the N-H stretching region (3150 – 3600 cm^{-1}),[10] a selection of which are shown in Figure 2a for different c_0 mixtures of 8tBA and T in chloroform. The spectra in Figure 2a contain bands that decrease with increasing c_0, which we assign to N-H and NH_2 stretching modes of monomeric 8tBA (3412, 3525 cm^{-1}) and T (3395 cm^{-1}),[29, 30] whereas features that grow with increasing c_0 are attributed to vibrations of 8tBA•T (3185, 3215, 3315, 3492 cm^{-1}),[29] in either configuration **1** or **2**. Following methods outlined previously,[10, 36] analysis of the spectra in Figure 2a returns the $\beta_{8tBA\bullet T}$ *vs* $\log(c_0)$ curve in Figure 2b (black data) and $K_{8tBA\bullet T}$ = 45 ± 3 M^{-1} (*cf.* $K_{A\bullet T}$ = 130 ± 13 M^{-1} [35]). Self-association constants for 8tBA•8tBA and T•T homodimers are both ≤ 3 M^{-1}.[30, 35]

Figure 3a displays TEA spectra for a c_0 = 50 mM mixture of 8tBA and T in chloroform, excited at λ = 260 nm. Chloroform solvent was selected as it both encourages H-bonding between 8tBA and T and offers a dielectric medium comparable to that experienced in the core of DNA helices.[37] Half of the mixture is present as 8tBA•T pairs in forms **1** and **2** ($\beta_{8tBA\bullet T}$ = 0.52), with the remainder present as monomers (N.B. homodimers make a minimal contribution to the mixture). Values of $c_0 \leq$ 50 mM were used to avoid formation of higher order H-bonding structures (*e.g.* trimers and ribbons).[38, 39] After excitation, the spectra are dominated by a structured excited state absorption (ESA) signal, arising from a combination of photo-excited 8tBA•T, 8tBA and T species. No obvious changes to the structure of the ESA profile are observed as it decays uniformly over time. The spectral profile is reminiscent of those observed for TEAS of 8tBA and T monomers in chloroform at 260 nm (c_0 = 50 mM), which are shown in panels b and c of Figure 3 for comparison. In the case of the monomers, the absorption profiles are similar to those reported previously for aqueous A and T,[40, 41] where the signal is assigned to ESA from an initially populated $^1\pi\pi^*$ state to higher lying singlet states (S_n). Unlike H-bonded aggregates of simpler heteroaromatic systems,[42] no new discernable features associated with residual 8tBA•8tBA ($\beta_{8tBA\bullet 8tBA} \leq 0.20$) and T•T ($\beta_{T\bullet T}$ = 0.15) homodimers are observed in chloroform.

Overlaid in Figure 3a are the absorption profiles of the A[–H] (red circles) and T[+H] (blue circles) radicals,[43, 44] both of which are key intermediates in the first suggested EDPT process along the $N_{6,8tBA}$–H···O_T coordinate[23] – see step **i** and 8tBA[–H]•T[+H] biradical structure (**5**) in Figure 1. Unlike the TEA spectra in Figure 3a, neither radical absorbs strongly at ~410 nm, nor steadily increases in absorbance at >600 nm. This observation leads us to conclude that, if EDPT is active in 8tBA•T pairs at 260 nm with a significant quantum yield, no local minimum exists along the driving $^1\pi\pi^*_{CT}$ state; this behavior differs from the analogous G[–H]•C[+H] biradical, which is transiently trapped on a $^1\pi\pi^*_{CT}$ surface for 2.9 ps.[14] Moreover, it implies that monomer-like relaxation pathways dominate in 8tBA•T pairs, consistent with the similar $S_n \leftarrow {}^1\pi\pi^*$ ESA profiles observed for the 8tBA + T mixture and the 8tBA and T monomers.

Figure 3d displays an ESA decay trace at λ_{probe} = 400 nm (circles). The majority of signal decays within ~1 ps, with a small fraction decaying over a several picosecond

timeframe. A minor amount of residual signal persists up to 1 ns. The ESA decay can be well modeled (black line) by a scaled linear sum of the monomer decay kinetics, extracted from independent TEAS on T (dashed blue) and 8tBA (dashed red), further hinting that relaxation dynamics of 8tBA•T pairs (*ca*. 50% of the mixture) are simply akin to those of the monomers. Although it is only a minor component (3%) of the fit in Figure 3d, T relaxation (Figure 3f) is found to occur with three time-constants: τ_{T1} < 40 fs, τ_{T2} = 890 ± 40 fs and $\tau_{T3} \geq 1.2$ ns. Based on prior theoretical calculations, we propose that τ_{T1} may arise from evolution of the excited wavepacket out of the vertical Franck-Condon (vFC) region,[30] although undesired contributions from a multi-photon solvent-only response cannot be ruled out.[45] Analogous to earlier studies of aqueous T, τ_{T2} reflects the lifetime of the initially excited $^1\pi\pi^*_T$ state.[41] After 260 nm excitation, population on $^1\pi\pi^*_T$ can either decay directly back to a vibrationally hot S_0 state (83%), *via* an ethylenic-twist type conical intersection,[6, 46] or undergo ultrafast internal conversion onto a near-isoenergetic $^1n_O\pi^*_T$ state (17%) in the vFC region.[30] Formation and decay of the dark $^1n_O\pi^*_T$ state in T is not detected in TEAS,[30, 47] although previous TVAS studies have revealed the $^1n_O\pi^*_T$ state lifetime to be ~114 ps in chloroform.[30] The $^1n_O\pi^*_T$ state also acts as a doorway to populating a long-lived $^3\pi\pi^*_T$ (T_1) state (τ > 1 ns), leading us to assign τ_{T3} to triplet state decay,[30, 48] with possible undesired contributions from $CHCl_3$ solvent only dynamics[45] (Figure S10).

The majority of ESA decay for the 8tBA + T mixture in Figure 3d is captured by 8tBA dynamics (97%). Although a greater fraction of 8tBA•T pairs is initially promoted into a locally excited $^1\pi\pi^*_{8tBA}$ state (~60%, Figure S9) than to the corresponding $^1\pi\pi^*_T$ state localized on T, this alone cannot account for the dominance of 8tBA dynamics in Figure 3d. We suggest that ultrafast $^1\pi\pi^*_T \rightarrow {}^1\pi\pi^*_{8tBA}$ coupling in 8tBA•T is unlikely, as this state transition requires two electrons. Alternatively, if complexation of T with 8tBA dramatically enhances ultrafast population transfer from $^1\pi\pi^*_T$ to $^1n_O\pi^*_T$ (*cf*. 17% in T monomers[30]), the measured TEA spectra will be dominated by signal from 8tBA, given that $^1n_O\pi^*_T$ is optically dark to ESA.[30, 47] However, further verification of this hypothesis requires detailed computational studies, which are beyond the scope of this current study. Exponential kinetic fits in Figure 3e show that 8tBA monomers relax with time-constants of τ_{A1} = 337 ± 14 fs, τ_{A2} = 4.4 ± 0.8 ps and $\tau_{A3} \geq 1.2$ ns. In accord

with earlier work on A,[31, 40, 41] τ_{A1} is attributed to the lifetime of the $^1\pi\pi^*_{8tBA}$ state, which is predicted to decay to S_0 *via* a conical intersection involving out-of-plane ring distortion at the C_2 site (Figure 1).[6] Unlike 8tBA in chloroform though, time-constants on the order of picoseconds and nanoseconds were not reported previously for aqueous A.[40, 41] There are a number of possible origins for these additional time-constants, which we briefly discuss. First, given that similar dynamics were observed for silyl-protected dA and 8tBA in chloroform (Figure S11), we discount any significant impact of the additional *t*-butyl group on 8tBA's relaxation dynamics. However, different solute-solvent interactions in chloroform *vs* water could modify the excited state potential energy landscape and open new relaxation channels. A notable candidate would be the assignment of τ_{A2} to relaxation *via* a $^1n_N\pi^*_{8tBA}$ state,[6, 49] given our previous findings that chloroform can stabilize states of $n\pi^*$ character in pyrimidine nucleosides, relative to more polar, protic solvents.[30] There is also evidence that the imino tautomer of 8tBA is present in chloroform (8tBA*, Figure S12), which may alternatively be associated with τ_{A2}; extended excited state lifetimes in minority nucleobase tautomers have been identified previously for 7H-adenine[31, 50, 51] and the imino tautomer of C.[30] Finally, likely candidates for τ_{A3} are either minor contributions from 8tBA•8tBA homodimers (*cf.* C•C homodimers[30]) or population of triplet states. In order to assign more definitively τ_{A2} and τ_{A3}, further complementary *ab initio* and dynamical simulations are required.

TVAS was used to probe for signatures of long-lived photoproducts and/or biradical intermediates arising from EDPT,[14] such as the imino-enol 8tBA*•T* tautomer pair (**6**) and 8tBA[–H]•T[+H] biradical (**5**). Figure 4a displays TVA spectra, recorded in the carbonyl stretching region, after λ = 260 nm excitation. Negative bleach signals that partially recover with time (~80%) are observed at 1638 (ν_{scis}, 8tBA and 8tBA•T), 1687 and 1705 cm^{-1} (ν_{CO}, T and 8tBA•T), reflecting $^1\pi\pi^* \leftarrow S_0$ population transfer. The locations of these bleaches match the inverted FTIR spectrum, which is composed of a linear sum of FTIR spectra for individual 8tBA (red), T (blue) and 8tBA•T (black) species (Figure 4b), given $\beta_{8tBA•T}$ = 0.52. Comparison of experimental and simulated (B3LYP/6-311++G**) FTIR spectra for 8tBA•T pairs show good agreement (Figure 4c), further supporting that 8tBA•T exists in forms **1** (67%) and **2** (33%). In addition to bleaches, Figure 4a contains positive features at 1600, 1612 and 1670 cm^{-1} that decay

and blue-shift with increasing time, indicative of nascent vibrationally hot S_0 species (ν*) that undergo cooling after ultrafast internal conversion back to their electronic ground states[31, 52] (*cf.* TEAS). A global fit analysis (see SI) of the data in Figure 4a returns the representative kinetic profiles in panel d. Exponential kinetic fits to the vibrational hot band decay (1612 cm^{-1}) and bleach recovery (1687 cm^{-1}) return a time constant of τ_{VC} = 10.1 ± 0.6 ps, which we interpret as an average, non-mode specific vibrational cooling timescale for 8tBA, T and 8tBA•T, due to the mixed nature of the sample.

Positive bands, which do not decay after their initial growth, are also observed at 1620 and 1720 cm^{-1} in the TVA spectra. These features arise from either photoproduct formation or population of long-lived intermediate states (*e.g.* triplets), in-line with incomplete bleach recovery up to t = 1.2 ns. DFT calculations predict that an imino-enol 8tBA*•T* photoproduct (**6**) should absorb strongly at ~1680 cm^{-1}, but does not possess a marker band at ~1720 cm^{-1} (Figure S6). This hints that, unlike WC G•C pairs,[14] an analogous stepwise double EDPT process (Figure 1, **i**-**iii**) may not be active in 8tBA•T pairs, although we acknowledge that overlap with bleach signals in this spectral region may obfuscate signatures for 8tBA*•T*. Additionally, calculated 8tBA•T triplet state vibrations do not match the observed product bands in TVAS (Figure S7). Instead, the most convincing assignment for the 1620 and 1720 cm^{-1} bands is simply to dynamics occurring in the residual 8tBA and T monomers. Figure 4e compares a t = 1.2 ns TVA spectrum of the equimolar mix (black), to those recorded in TVAS on 8tBA (red) and T (blue) monomers – see SI.[30] Within error, the sum of the 8tBA and T only spectra (dashed line) reproduces the observed 1.2 ns spectrum for the 8tBA + T mixture; residual differences may be due to incomplete recovery of 8tBA•T pairs, although a more detailed assignment would be unduly speculative. For T, we have recently assigned delayed appearance and build-up of features at 1720 and 1600–1650 cm^{-1} to $^3\pi\pi^*_T$ (T_1) formation,[30] in-line with the kinetics (τ = 16 ± 4 ps) of the 1720 cm^{-1} band here (Figure 4d). For 8tBA, DFT calculations (Figure S8) predict that product bands at 1620 and 1690 cm^{-1} likely arise from photo-induced 8tBA → 8tBA* tautomerization,[53] with the 1620 cm^{-1} feature giving rise to the observed long-time signal offset in the kinetic trace of the overlapping hot band at 1612 cm^{-1} (Figure 4d).

4. Discussion

Previous TEAS and TVAS studies of WC G•C pairs provided compelling evidence for sequential EDPT dynamics.[14] However, analogous measurements here do not yield similarly clear signatures of EDPT in a chemically modified A•T base pair. Despite successful elimination of Hoogsteen motifs (**3**,**4**) through a *t*-butyl group at C_8 of A, the lower association constant for 8tBA•T ($K_{8tBA•T}$ = 45 M^{-1}), relative to G•C ($K_{G•C}$ = 3.4 × 10^4 M^{-1}),[10] still leads to a complex sample mixture at c_0 values appropriate for TEAS and TVAS. Nonetheless, a number of conclusions can still be drawn from these measurements, which we herein discuss with relation to: (i) theoretically proposed EDPT pathways for A•T,[5, 22-27] summarized in Figure 1; and (ii) previously observed EDPT in G•C.[14]

No clear spectroscopic evidence for a double H-atom transferred 8tBA*•T* photoproduct (**6**) was observed in TVAS, leading us to suggest that EDPT processes **ii**-**iv** are unlikely to be active with any significant quantum yield in UV-excited 8tBA•T; all TVAS photoproduct bands can be rationalized in terms of residual monomer dynamics. The non-observation of 8tBA*•T* is also in accord with computations by Gorb *et al.* on A•T,[28] which predict that, although bound with respect to potential energy,[22, 23, 28] A*•T* tautomers are not stable in Gibbs free energy space. This behavior contrasts both theoretical predictions and experimental findings for G•C, which together show that the corresponding G*•C* tautomer can be generated through a two-step EDPT mechanism and is subsequently stable on a timeframe of ≥ 1 ns.[14, 21, 28]

In TEAS on G•C, clear spectroscopic signatures were observed for a G[–H]•C[+H] biradical, formed *via* EDPT.[14] No analogous signatures for 8tBA[–H]•T[+H] are captured in TEAS on 8tBA•T. To rationalize this observation, we draw upon previous theoretical studies of EDPT in A•T, in both the gas-phase[5, 22-27] and aqueous solution.[26] A number of prior computations collectively suggest that, for isolated A•T WC pairs, the $^1\pi\pi^*_{CT}$ state responsible for EDPT is significantly less stable in the vFC region, compared to G•C.[5, 6, 22, 23, 26] This behavior creates a ≤0.8 eV barrier to coupling from the adiabatic minimum of the lowest energy, locally excited $^1\pi\pi^*$ state onto the $^1\pi\pi^*_{CT}$ surface,[5, 22, 23] hindering population of $^1\pi\pi^*_{CT}$, and favoring ultrafast monomer-like

relaxation pathways.[6, 27] Additionally, the calculated potential energy profile of $^1\pi\pi^*_{CT}$ along the EDPT coordinate of isolated A•T (*cf*. steps **i** and **v**, Figure 1) is purely repulsive, preventing any biradical species from being temporarily trapped en route to the $^1\pi\pi^*_{CT}/S_0$ conical intersection.[5, 22, 23, 27] Gas-phase spectroscopy measurements on A•T WC pairs are still required to confirm these predictions.[6] In contrast, computational modelling of A•T WC pairs in aqueous solution predicts significant stabilization of $^1\pi\pi^*_{CT}$, becoming the lowest energy singlet excited state, and the formation of a local minimum in the vicinity of the biradical structure, prior to the $^1\pi\pi^*_{CT}/S_0$ conical intersection.[6, 26] When combined, these factors enhance the probability for UV-induced EDPT and spectroscopic detection of a biradical intermediate in aqueous A•T WC pairs, relative to the gas-phase.[6]

It is unlikely that the excited state relaxation dynamics of our model 8tBA•T WC pairs in chloroform rigorously conform to the scenarios predicted for aqueous or isolated A•T WC pairs. Nonetheless, based on the absence of any signatures for 8tBA[–H]•T[+H] and EDPT in TEAS, we propose that the UV-induced dynamics of 8tBA•T in chloroform are more akin to those predicted for A•T in the gas-phase, suggesting that: (i) monomer-like dynamics dominate in 8tBA•T; and (ii) relative to water, chloroform is not as effective at stabilizing the $^1\pi\pi^*_{CT}$ state. However, a caveat is required; if EDPT processes **i** and **v** are both active and complete on a sub-100 fs timeframe, akin to the hypothesized photoprotection mechanism of Perun *et al*.,[5] then our TEAS measurements will be unable to resolve kinetically these dynamics in 8tBA•T (*cf*. IRF ~ 110 fs). It is therefore not possible for us to rule out completely the participation of ultrafast EDPT *via* pathways **i** and **v**.

5. Conclusions

Our present TEAS and TVAS measurements offer the first experimental insights into the UV-induced dynamics of a solvated A•T base pair, through the use of a chemically modified adenine derivative, 8tBA. With the potential caveat of a possible, but unobservable, ultrafast (sub-100 fs) EDPT mechanism, we propose that, unlike G•C WC pairs,[14] monomer-like dynamics[27] dominate in the relaxation of 8tBA•T pairs (and by heuristic extension, A•T pairs). Prior theoretical calculations predict these

monomer-like pathways to involve conical intersections along ethylenic C=C twisting (T) and out-of-plane ring distortion (8tBA) coordinates.[6, 27] Despite elimination of Hoogsteen motifs, the low association constant for 8tBA•T prohibits exclusive probing of the dynamics in WC pairs, and some interference from monomer photochemistry contributes to our measurements. In order to alleviate this issue, future work could conceivably utilize alternative synthetic and spectroscopic techniques, such as covalently tethering 8tBA and T together with a flexible aliphatic linker[54, 55] or *transient* two-dimensional infrared spectroscopy[56] of 8tBA•T to disentangle monomer and base pair dynamics.

Acknowledgements

The authors are grateful to Dr Craig Butts for assistance with recording and analysing NMR data. KR thanks the Deutsche Forschungsgemeinschaft for a Research Fellowship. HJBM thanks the EPSRC for the award of a Doctoral Training Grant studentship. EE thanks the Royal Society of Chemistry for a summer student bursary. TAAO is funded by a Royal Society University Research Fellowship (UF140231). STGS and ASH thank EPSRC EP/G036764/1 for their CDT Ph.D. studentships. MCG thanks the EPSRC EP/J002542/1 for funding. GMR acknowledges the Ramsay Memorial Trust for the award of a Ramsay Memorial Fellowship. This work was supported by the European Research Council through the ERC Advanced Grant 290966 CAPRI.

Supporting Information

Synthesis details, characterization through NMR and 2DIR spectra, calculation of dimer fractions, summary of vibrational mode labels, calculated photoproduct spectra, steady-state UV/visible absorption spectra, solvent only TEAS measurements, comparison of dA and 8tBA dynamics, TVAS global fitting details. This material is available free of charge *via* the Internet at http://pubs.acs.org. The raw data supporting this article can be accessed online at: http://dx.doi.org/10.5523/bris.xyjoxo6lkca412cqoqyipk5i5.

References

(1) Löwdin, P. O. Proton Tunneling in DNA and Its Biological Implications. *Rev. Mod. Phys.* **1963,** *35*, 724-732.

(2) Cukier, R. I.; Nocera, D. G. Proton-coupled electron transfer. *Annu. Rev. Phys. Chem.* **1998,** *49*, 337-369.

(3) Sobolewski, A. L.; Domcke, W. Ab initio studies on the photophysics of the guanine-cytosine base pair. *Phys. Chem. Chem. Phys.* **2004,** *6*, 2763-2771.

(4) Sobolewski, A. L.; Domcke, W.; Hattig, C. Tautomeric selectivity of the excited-state lifetime of guanine/cytosine base pairs: The role of electron-driven proton-transfer processes. *Proc. Natl. Acad. Sci. USA* **2005,** *102*, 17903-17906.

(5) Perun, S.; Sobolewski, A. L.; Domcke, W. Role of electron-driven proton-transfer processes in the excited-state deactivation adenine-thymine base pair. *J. Phys. Chem. A* **2006,** *110*, 9031-9038.

(6) Improta, R.; Santoro, F.; Blancafort, L. Quantum Mechanical Studies on the Photophysics and the Photochemistry of Nucleic Acids and Nucleobases. *Chem. Rev.* **2016,** *116*, 3540-3593.

(7) Crespo-Hernandez, C. E.; Cohen, B.; Hare, P. M.; Kohler, B. Ultrafast excited-state dynamics in nucleic acids. *Chem. Rev.* **2004,** *104*, 1977-2019.

(8) Middleton, C. T.; de La Harpe, K.; Su, C.; Law, Y. K.; Crespo-Hernandez, C. E.; Kohler, B. DNA Excited-State Dynamics: From Single Bases to the Double Helix. *Annu. Rev. Phys. Chem.* **2009,** *60*, 217-239.

(9) Schreier, W. J.; Gilch, P.; Zinth, W. Early Events of DNA Photodamage. *Annu. Rev. Phys. Chem.* **2015,** *66*, 497-519.

(10) Schwalb, N. K.; Michalak, T.; Temps, F. Ultrashort Fluorescence Lifetimes of Hydrogen-Bonded Base Pairs of Guanosine and Cytidine in Solution. *J. Phys. Chem. B* **2009,** *113*, 16365-16376.

(11) Biemann, L.; Kovalenko, S. A.; Kleinermanns, K.; Mahrwald, R.; Markert, M.; Improta, R. Excited State Proton Transfer Is Not Involved in the Ultrafast Deactivation of Guanine-Cytosine Pair in Solution. *J. Am. Chem. Soc.* **2011,** *133*, 19664-19667.

(12) Bucher, D. B.; Schlueter, A.; Carell, T.; Zinth, W. Watson-Crick Base Pairing Controls Excited-State Decay in Natural DNA. *Angew. Chem. Int. Ed.* **2014,** *53*, 11366-11369.

(13) Zhang, Y. Y.; de La Harpe, K.; Beckstead, A. A.; Improta, R.; Kohler, B. UV-Induced Proton Transfer between DNA Strands. *J. Am. Chem. Soc.* **2015,** *137*, 7059-7062.

(14) Rottger, K.; Marroux, H. J. B.; Grubb, M. P.; Coulter, P. M.; Bohnke, H.; Henderson, A. S.; Galan, M. C.; Temps, F.; Orr-Ewing, A. J.; Roberts, G. M. Ultraviolet Absorption Induces Hydrogen-Atom Transfer in G-C Watson-Crick DNA Base Pairs in Solution. *Angew. Chem. Int. Ed.* **2015,** *54*, 14719-14722.

(15) Zhang, Y. Y.; de La Harpe, K.; Beckstead, A. A.; Martinez-Fernandez, L.; Improta, R.; Kohler, B. Excited-State Dynamics of DNA Duplexes with Different H-Bonding Motifs. *J. Phys. Chem. Lett.* **2016,** *7*, 950-954.

(16) Zhang, Y. Y.; Li, X. B.; Fleming, A. M.; Dood, J.; Beckstead, A. A.; Orendt, A. M.; Burrows, C. J.; Kohler, B. UV-Induced Proton-Coupled Electron Transfer in Cyclic DNA Miniduplexes. *J. Am. Chem. Soc.* **2016,** *138*, 7395-7401.

(17) Schwalb, N. K.; Temps, F. Ultrafast electronic relaxation in guanosine is promoted by hydrogen bonding with cytidine. *J. Am. Chem. Soc.* **2007,** *129*, 9272-9273.

(18) Abo-Riziq, A.; Grace, L.; Nir, E.; Kabelac, M.; Hobza, P.; de Vries, M. S. Photochemical selectivity in guanine-cytosine base-pair structures. *Proc. Natl. Acad. Sci. USA* **2005,** *102*, 20-23.

(19) Groenhof, G.; Schafer, L. V.; Boggio-Pasqua, M.; Goette, M.; Grubmuller, H.; Robb, M. A. Ultrafast deactivation of an excited cytosine-guanine base pair in DNA. *J. Am. Chem. Soc.* **2007,** *129*, 6812-6819.

(20) Yamazaki, S.; Taketsugu, T. Photoreaction channels of the guanine-cytosine base pair explored by long-range corrected TDDFT calculations. *Phys. Chem. Chem. Phys.* **2012,** *14*, 8866-8877.

(21) Sauri, V.; Gobbo, J. P.; Serrano-Perez, J. J.; Lundberg, M.; Coto, P. B.; Serrano-Andres, L.; Borin, A. C.; Lindh, R.; Merchan, M.; Roca-Sanjuan, D. Proton/Hydrogen Transfer Mechanisms in the Guanine-Cytosine Base Pair: Photostability and Tautomerism. *J. Chem. Theory Comput.* **2013,** *9*, 481-496.

(22) Ai, Y. J.; Zhang, F.; Cui, G. L.; Luo, Y.; Fang, W. H. Ultrafast deactivation processes in the 2-aminopyridine dimer and the adenine-thymine base pair: Similarities and differences. *J. Chem. Phys.* **2010,** *133*, 064302.

(23) Gobbo, J. P.; Sauri, V.; Roca-Sanjuan, D.; Serrano-Andres, L.; Merchan, M.; Borin, A. C. On the Deactivation Mechanisms of Adenine-Thymine Base Pair. *J. Phys. Chem. B* **2012,** *116*, 4089-4097.

(24) Alexandrova, A. N.; Tully, J. C.; Granucci, G. Photochemistry of DNA Fragments via Semiclassical Nonadiabatic Dynamics. *J. Phys. Chem. B* **2010,** *114*, 12116-12128.
(25) Jensen, L.; Govind, N. Excited States of DNA Base Pairs Using Long-Range Corrected Time-Dependent Density Functional Theory. *J. Phys. Chem. A* **2009,** *113*, 9761-9765.
(26) Dargiewicz, M.; Biczysko, M.; Improta, R.; Barone, V. Solvent effects on electron-driven proton-transfer processes: adenine-thymine base pairs. *Phys. Chem. Chem. Phys.* **2012,** *14*, 8981-8989.
(27) Marchetti, B.; Karsili, T. N. V.; Ashfold, M. N. R.; Domcke, W. A 'bottom up', ab initio computational approach to understanding fundamental photophysical processes in nitrogen containing heterocycles, DNA bases and base pairs. *Phys. Chem. Chem. Phys.* **2016,** *18*, 20007-20027.
(28) Gorb, L.; Podolyan, Y.; Dziekonski, P.; Sokalski, W. A.; Leszczynski, J. Double-proton transfer in Adenine-Thymine and Guanine-Cytosine base pairs. A post-hartree-fock ab initio study. *J. Am. Chem. Soc.* **2004,** *126*, 10119-10129.
(29) Greve, C.; Preketes, N. K.; Fidder, H.; Costard, R.; Koeppe, B.; Heisler, I. A.; Mukamel, S.; Temps, F.; Nibbering, E. T. J.; Elsaesser, T. N-H Stretching Excitations in Adenosine-Thymidine Base Pairs in Solution: Pair Geometries, Infrared Line Shapes, and Ultrafast Vibrational Dynamics. *J. Phys. Chem. A* **2013,** *117*, 594-606.
(30) Rottger, K.; Marroux, H. J. B.; Bohnke, H.; Morris, D. T. J.; Voice, A. T.; Temps, F.; Roberts, G. M.; Orr-Ewing, A. J. Probing the Excited State Relaxation Dynamics of Pyrimidine Nucleosides in Chloroform Solution. *Faraday Discuss.* **2016,** *194*, 683-708.
(31) Roberts, G. M.; Marroux, H. J. B.; Grubb, M. P.; Ashfold, M. N. R.; Orr-Ewing, A. J. On the Participation of Photoinduced N-H Bond Fission in Aqueous Adenine at 266 and 220 nm: A Combined Ultrafast Transient Electronic and Vibrational Absorption Spectroscopy Study. *J. Phys. Chem. A* **2014,** *118*, 11211-11225.
(32) Frisch, M. J.; Trucks, G. W.; Schlegel, H. B.; Scuseria, G. E.; Robb, M. A.; Cheeseman, J. R.; Scalmani, G.; Barone, V.; Mennucci, B.; Petersson, G. A., *et al. Gaussian 09*; Gaussian Inc.: Wallingford, CT, 2009.
(33) Chen, M. C.; Lord, R. C. Reinvestigation of Specific Hydrogen-Bonding of Certain Adenine and Uracil Derivatives by Infrared Spectroscopy. *Biochim. Biophys. Acta* **1974,** *340*, 90-94.
(34) Woutersen, S.; Cristalli, G. Strong enhancement of vibrational relaxation by Watson-Crick base pairing. *J. Chem. Phys.* **2004,** *121*, 5381-5386.

(35) Kyogoku, Y.; Lord, R. C.; Rich, A. Effect of Substituents on Hydrogen Bonding of Adenine and Uracil Derivatives. *Proc. Natl. Acad. Sci. USA* **1967,** *57*, 250-257.

(36) Kyogoku, Y.; Lord, R. C.; Rich, A. An Infrared Study of Hydrogen Bonding between Adenine and Uracil Derivatives in Chloroform Solution. *J. Am. Chem. Soc.* **1967,** *89*, 496-504.

(37) Siriwong, K.; Voityuk, A. A.; Newton, M. D.; Rosch, N. Estimate of the reorganization energy for charge transfer in DNA. *J. Phys. Chem. B* **2003,** *107*, 2595-2601.

(38) Schwalb, N. K.; Temps, F. On the structure and excited electronic state lifetimes of cytidine self-assemblies with extended hydrogen-bonding networks. *J. Photochem. Photobiol. A* **2009,** *208*, 164-170.

(39) Biemann, L.; Haber, T.; Maydt, D.; Schaper, K.; Kleinermanns, K. Structural assignment of adenine aggregates in $CDCl_3$. *J. Chem. Phys.* **2008,** *128*, 195103.

(40) Pecourt, J. M. L.; Peon, J.; Kohler, B. Ultrafast internal conversion of electronically excited RNA and DNA nucleosides in water. *J. Am. Chem. Soc.* **2000,** *122*, 9348-9349.

(41) Pecourt, J. M. L.; Peon, J.; Kohler, B. DNA excited-state dynamics: Ultrafast internal conversion and vibrational cooling in a series of nucleosides. *J. Am. Chem. Soc.* **2001,** *123*, 10370-10378.

(42) Zhang, Y. Y.; Oliver, T. A. A.; Ashfold, M. N. R.; Bradforth, S. E. Contrasting the excited state reaction pathways of phenol and para-methylthiophenol in the gas and liquid phases. *Faraday Discuss.* **2012,** *157*, 141-163.

(43) Ito, T.; Kuno, S.; Uchida, T.; Fujita, S.; Nishimoto, S. Properties and Reactivity of the Adenosine Radical Generated by Radiation-Induced Oxidation in Aqueous Solution. *J. Phys. Chem. B* **2009,** *113*, 389-394.

(44) Hayon, E. Optical-Absorption Spectra of Ketyl Radicals and Radical Anions of Some Pyrimidines. *J. Chem. Phys.* **1969,** *51*, 4881-4892.

(45) Abou-Chahine, F.; Preston, T. J.; Dunning, G. T.; Orr-Ewing, A. J.; Greetham, G. M.; Clark, I. P.; Towrie, M.; Reid, S. A. Photoisomerization and Photoinduced Reactions in Liquid CCl_4 and $CHCl_3$. *J. Phys. Chem. A* **2013,** *117*, 13388-13398.

(46) Lan, Z. G.; Fabiano, E.; Thiel, W. Photoinduced Nonadiabatic Dynamics of Pyrimidine Nucleobases: On-the-Fly Surface-Hopping Study with Semiempirical Methods. *J. Phys. Chem. B* **2009,** *113*, 3548-3555.

(47) Hare, P. M.; Crespo-Hernandez, C. E.; Kohler, B. Internal conversion to the electronic ground state occurs via two distinct pathways for pyrimidine bases in aqueous solution. *Proc. Natl. Acad. Sci. USA* **2007,** *104*, 435-440.

(48) Hare, P. M.; Middleton, C. T.; Mertel, K. I.; Herbert, J. M.; Kohler, B. Time-resolved infrared spectroscopy of the lowest triplet state of thymine and thymidine. *Chem. Phys.* **2008,** *347*, 383-392.

(49) Serrano-Andres, L.; Merchan, M.; Borin, A. C. A three-state model for the photophysics of adenine. *Chem. Eur. J.* **2006,** *12*, 6559-6571.

(50) Marian, C. M.; Kleinschmidt, M.; Tatchen, J. The photophysics of 7H-adenine: A quantum chemical investigation including spin-orbit effects. *Chem. Phys.* **2008,** *347*, 346-359.

(51) Cohen, B.; Hare, P. M.; Kohler, B. Ultrafast excited-state dynamics of adenine and monomethylated adenines in solution: Implications for the nonradiative decay mechanism. *J. Am. Chem. Soc.* **2003,** *125*, 13594-13601.

(52) Murdock, D.; Harris, S. J.; Luke, J.; Grubb, M. P.; Orr-Ewing, A. J.; Ashfold, M. N. R. Transient UV Pump-IR Probe Investigation of Heterocyclic Ring-Opening Dynamics in the Solution Phase: The Role Played by nσ* States in the Photoinduced Reactions of Thiophenone and Furanone. *Phys. Chem. Chem. Phys.* **2014,** *16*, 21271-21279.

(53) Kwiatkowski, J. S.; Leszczynski, J. An Abinitio Quantum-Mechanical Study of Tautomerism of Purine, Adenine and Guanine. *J. Mol. Struct. (THEOCHEM)* **1990,** *67*, 35-44.

(54) Hocek, M.; Dvorak, D.; Havelkova, M. Covalent analogues of nucleobase-pairs. *Nucleos. Nucleot. Nucl.* **2003,** *22*, 775-777.

(55) Chen, J. Q.; Thazhathveetil, A. K.; Lewis, F. D.; Kohler, B. Ultrafast Excited-State Dynamics in Hexaethyleneglycol-Linked DNA Homoduplexes Made of A.T Base Pairs. *J. Am. Chem. Soc.* **2013,** *135*, 10290-10293.

(56) Bredenbeck, J.; Helbing, J.; Behrendt, R.; Renner, C.; Moroder, L.; Wachtveitl, J.; Hamm, P. Transient 2D-IR spectroscopy: Snapshots of the nonequilibrium ensemble during the picosecond conformational transition of a small peptide. *J. Phys. Chem. B* **2003,** *107*, 8654-8660.

Table 1. Calculated relative energies (ΔE) and Boltzmann populations at 298 K (P_B) for configurations **1-4** of 8tBA•T, and comparison to A•T, in $CHCl_3$. Calculations were performed at the B3LYP/6-311++G** level of theory using a chloroform PCM.

	8tBA•T		A•T	
Structure	ΔE / cm^{-1}	P_B (298 K)	ΔE / cm^{-1}	P_B (298 K)
WC (**1**)	0	62.1 %	161	19.4 %
reverse WC (**2**)	107	37.0 %	277	11.1 %
Hoogsteen (**3**)	889	0.9 %	0	42.3 %
reverse Hoogsteen (**4**)	1366	0.1 %	92	27.2 %

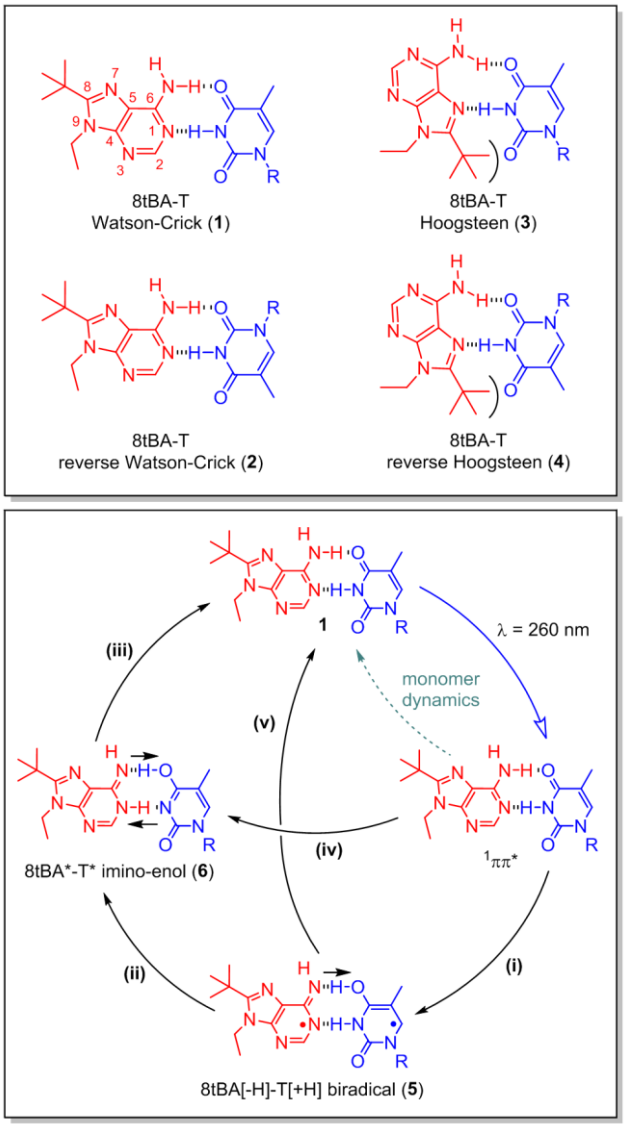

Figure 1. Upper panel: Possible H-bonding configurations for 8tBA•T pairs in chloroform (**1-4**), R = 3',5'-di-*O*-(*t*-butyldimethylsilyl)-2'-deoxy-ribose. **Lower panel**: Five theoretically proposed UV-induced EDPT pathways (**i-v**) for structure **1** of 8tBA•T, after excitation to the $^1\pi\pi^*_{8tBA}$ state, proceeding *via* the 8tBA[–H]•T[+H] biradical (**5**) and/or the 8tBA*•T* imino-enol tautomer (**6**). Monomer-like relaxation dynamics from $^1\pi\pi^*$ are indicated by the dashed grey arrow.

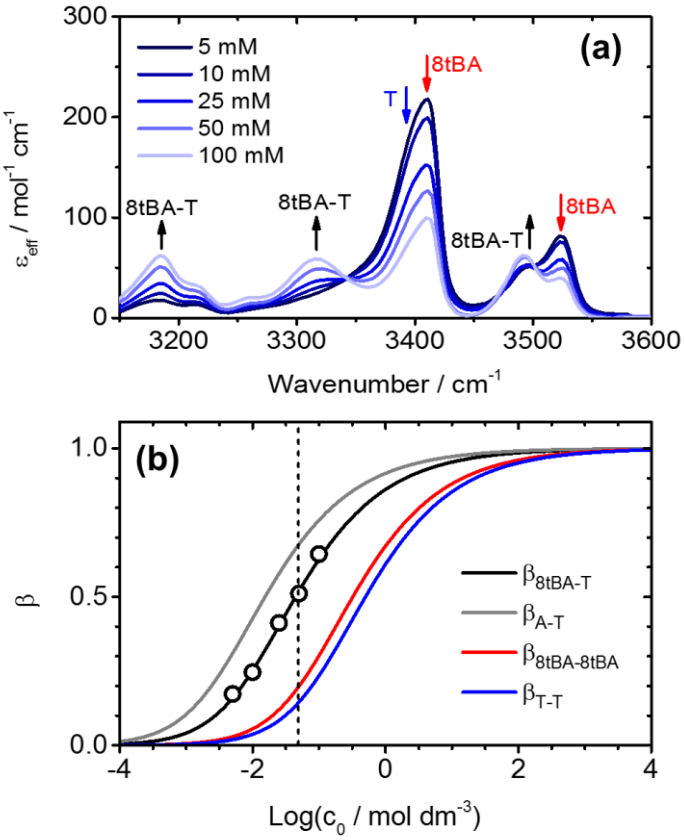

Figure 2. (a) Concentration (c_0) dependent steady-state FTIR spectra for equimolar mixtures of 8tBA and T in chloroform, recorded in the N-H stretching spectral region (3150 – 3600 cm^{-1}). **(b)** β *vs* log(c_0) curves (solid lines) for association into 8tBA•T (black), 8tBA•8tBA (red), T•T (blue) and A•T (grey), based on association equilibrium constants of $K_{8tBA•T}$ = 45 M^{-1}, $K_{8tBA•8tBA} \leq 3.1$ M^{-1}, $K_{T•T}$ = 2 M^{-1} and $K_{A•T}$ = 130 M^{-1}. Open circles indicate experimentally extracted $\beta_{8tBA•T}$ values obtained from analysis of FTIR spectra in (a). Vertical dashed line indicates $\beta_{M•N}$ for a value of c_0 = 50 mM.

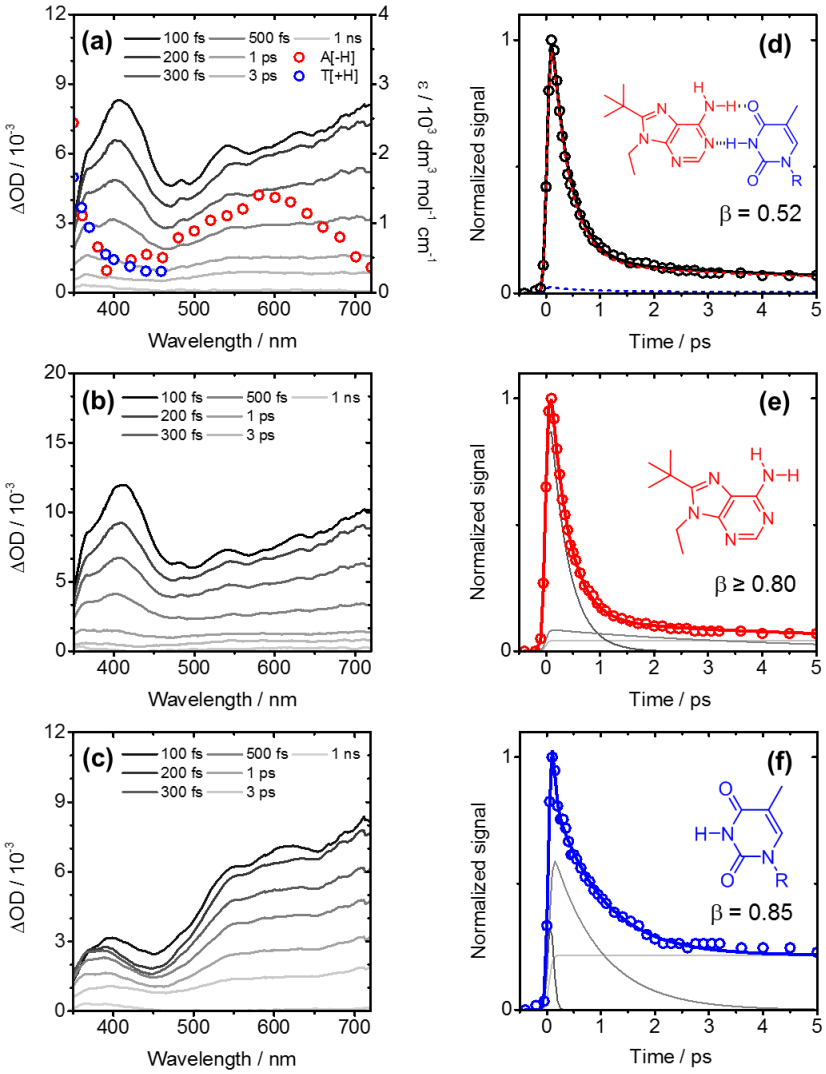

Figure 3. TEA spectra recorded in chloroform, after 260 nm excitation of **(a)** an equimolar mixture of 8tBA + T, **(b)** 8tBA and **(c)** T, where c_0 = 50 mM. (a) includes the absorption profiles for A[–H] (red circles) and T[+H] (blue circles) radicals.[43, 44] ESA decay profiles at λ_{probe} = 400 nm (circles) and kinetic fits (solid line) for **(d)** 8tBA + T, **(e)** 8tBA and **(f)** T. Data in (d) is fitted using a scaled linear sum of the independent kinetic fits to the T (dashed blue) and 8tBA (dashed red) monomer decay traces in (e) and (f). Grey lines in (e) and (f) show individual components of the tri-exponential fits to T ESA decay (τ_{T1} < 40 fs, τ_{T2} = 890 ± 40 fs, $\tau_{T3} \geq$ 1.2 ns) and 8tBA ESA decay (τ_{A1} = 337 ± 14 fs, τ_{A2} = 4.4 ± 0.8 ps, $\tau_{A3} \geq$ 1.2 ns).

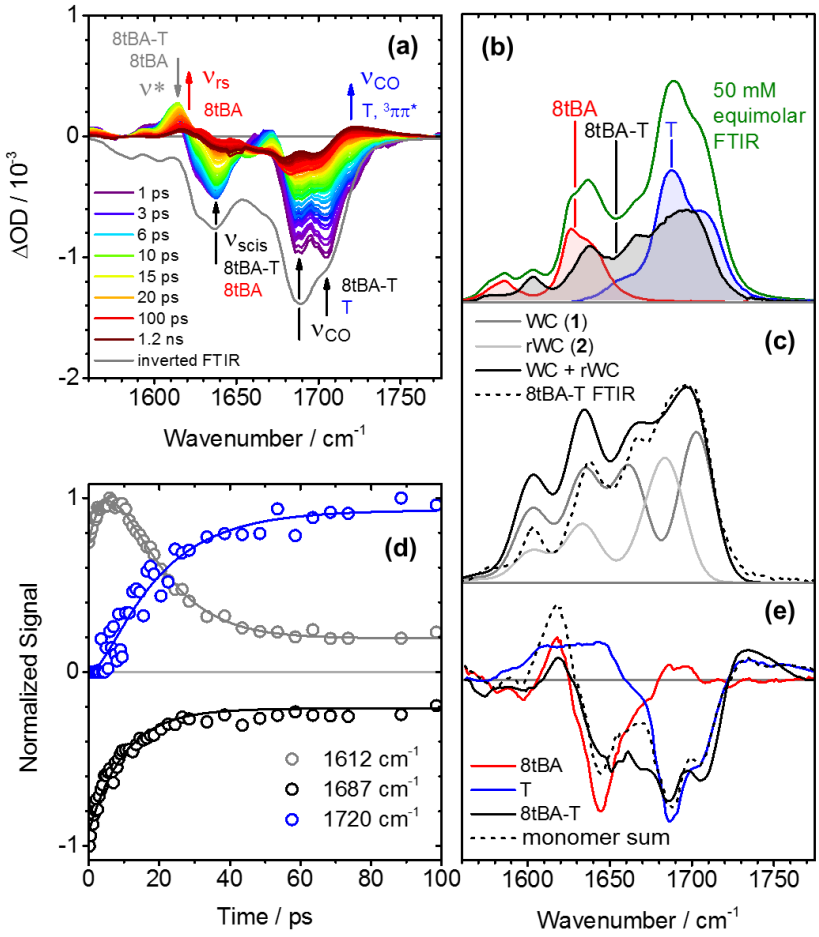

Figure 4. (a) TVA spectra recorded in the carbonyl stretching region, after 260-nm excitation of an equimolar mixture of 8tBA and T in chloroform (c_0 = 50 mM, $\beta_{8tBA\bullet T}$ = 0.52). See Table S2 in SI for vibrational mode labels. **(b)** Steady-state FTIR spectra for an equimolar mixture of 8tBA + T in chloroform (green), decomposed into contributions from 8tBA (red) and T (blue) monomers and 8tBA•T pairs (black), based on $\beta_{8tBA\bullet T}$ = 0.52. **(c)** Experimentally extracted FTIR spectrum for 8tBA•T pairs (dashed black) and calculated IR spectrum (black) composed of a 67:33 mixture of configurations **1** (dark grey) and **2** (light grey), respectively. **(d)** Kinetic traces (circles) and fits (lines) for representative bleach (black), ν* hot band (grey) and product features (blue). **(e)** Comparison of TVA spectra recorded at *t* = 1.2 ns for an equimolar mixture of 8tBA + T (black) and T (blue) and 8tBA (red) monomers.

TOC Graphic